Signature of tilted Dirac cones in Weiss oscillations of 8-*Pmmn* borophene

SK Firoz Islam* and A. M. Jayannavar†
Institute of Physics, Sachivalaya Marg, Bhubaneswar-751005, India
(Received 17 August 2017; revised manuscript received 20 October 2017; published 5 December 2017)

Polymorph of 8-*Pmmn* borophene exhibits anisotropic tilted Dirac cones. In this work, we explore the consequences of the tilted Dirac cones in magnetotransport properties of a periodically modulated borophene. We evaluate modulation-induced diffusive conductivity by using linear response theory in low temperature regime. The application of weak spatial modulation (electric, magnetic or both) gives rise to the magnetic-field-dependent nonzero oscillatory drift velocity which causes Weiss oscillation in the longitudinal conductivity at low magnetic field. The Weiss oscillation is studied in the presence of a weak spatial electric, magnetic, and both modulations individually. The tilting of the Dirac cones gives rise to an additional contribution to the Weiss oscillation in longitudinal conductivity. Moreover, it also enhances the frequency of the Weiss oscillation and modifies its amplitude too. Most remarkably, it is found that the presence of both out-of-phase electric and magnetic modulations can cause a sizable valley polarization in diffusive conductivity. The origin of valley polarization lies in the opposite tilting of the two Dirac cones at two valleys.

DOI: 10.1103/PhysRevB.96.235405

I. INTRODUCTION

In recent times, Dirac materials have attracted intense research interests after the most celebrated discovery of atomically thin two-dimensional (2D) hexagonal carbon allotrope graphene [1,2], owing to their peculiar band structure and applications in next generation of nanoelectronics. The polymorph of borophene with tilted anisotropic Dirac cones (named as 8-*Pmmn* borophene) [3] is the latest 2D material to the family of Dirac systems. Very recently, experimental confirmation of such material has been reported [4], followed by a detailed analysis of its *ab initio* properties [5]. Similar to the strained graphene [6], a pseudomagnetic field has been recently predicted in 8-*Pmmn* borophene by using a tight-binding model [7]. An effective low-energy Hamiltonian in the vicinity of Dirac points has been proposed based on symmetry consideration [7], which has recently been used to investigate collective excitations (plasmons) [8] and optical properties [9] theoretically.

Magnetotransport properties have always been appreciated for providing a powerful and experimentally reliable tool to probe a 2D fermionic system. The presence of a magnetic field, normal to the plane of the 2D sheet of an electronic system, discretizes the energy spectrum by forming Landau levels (LLs) which manifests itself via oscillatory longitudinal conductivity with an inverse magnetic field known as Shubnikov–de Hass (SdH) oscillation [10,11]. In addition to the SdH oscillation, another type of quantum oscillations appears in the low magnetic field regime when the 2D fermionic system is subjected to a weak spatial electric/magnetic modulation. This oscillation is known as Weiss oscillation, which was first observed in magnetoresistance measurements in the electrically modulated usual two-dimensional electron gas (2DEG) [12–14]. The Weiss oscillation is also known as commensurability oscillation as it is caused by the commensurability of the two length scales, i.e., cyclotron orbit's radius near the Fermi energy and the modulation period [15–17]. An alternative explanation was also given by Beenakker [18] by using the concept of *guiding-center-drift resonance* between the periodic cyclotron orbit motion and the oscillating drift of the orbit center induced by the potential grating.

Apart from the electric modulation case, magnetic modulation has also been considered theoretically [19–25] as well as experimentally [26–28]. Weiss oscillation has been studied in Rashba spin-orbit-coupled electrically/magnetically modulated 2DEG and a beating pattern was predicted [29,30]. The higher Fermi velocity associated with the linear band dispersion significantly enhances the Weiss oscillation in an electrically modulated graphene [31,32]. Concurrently, the same has been studied in a magnetically modulated graphene, too, and enhancement of the amplitude and opposite phase in comparison to the case of electrically modulated graphene was observed [33]. Similar investigations have been carried out in electrically modulated bilayer graphene [34], silicene [35,36], α-$\mathcal{T}_3$ lattice [37], and phosphorene [38]. However, magnetotransport properties of modulated borophene are yet to be explored.

In this work, we investigate the modulation-induced longitudinal conductivity of borophene in low temperature regime by using the linear response theory. First, we obtain exact LLs and corresponding density of states (DOS) in 8-*Pmmn* borophene. Numerically, we notice that the tilting of the Dirac cones lowers the Fermi level. We observe modulation-induced Weiss oscillation in the longitudinal conductivity in low magnetic field regime. Interestingly, we find that the opposite tilting of the Dirac cones at two valleys can cause sizable valley polarization in the longitudinal conductivity at low magnetic field regime under the combined effects of out-of-phase electric and magnetic modulation, which is in contrast to the nontilted isotropic Dirac cones graphene. Moreover, the tilting of the Dirac cones also enhances the frequency of Weiss oscillation.

The paper is organized as follows. In Sec. II, we introduce the low-energy effective Hamiltonian and derive LLs. The effect of tilting of Dirac cones on the Fermi level and DOS are also included in this section. Section III is devoted to

*firoz@iopb.res.in
†jayan@iopb.res.in

calculating the modulation-induced Weiss oscillation in the longitudinal conductivity. Finally, we summarize and conclude in Sec. IV.

II. MODEL HAMILTONIAN AND LANDAU LEVEL FORMATION

We start with the single-particle low-energy effective model Hamiltonian of the tilted anisotropic Dirac cones as [7,8]

$$H = \xi(v_x p_x\sigma_x + v_y p_y\sigma_y + v_t p_y\sigma_0), \tag{1}$$

where the first two terms correspond to the kinetic energy term and the last term describes the tilted nature of Dirac cones. The two Dirac points are at $\mathbf{k} = \pm\mathbf{k_D}$, described by the valley index $\xi = \pm$. Hereafter, we shall denote two valleys as K and K', corresponding to $\xi = +$ and $\xi = -$, respectively. Three velocities are given by $\{v_x,v_y,v_t\} = \{0.86,0.69,0.32\}$ in units of $v_0 = 10^6$ m/s. The velocity v_t arises due to the tilting of the Dirac cones. Also, (σ_x,σ_y) are the Pauli matrices and σ_0 is identity matrix. The energy dispersion of the above Hamiltonian can be readily obtained as

$$E^{\xi}_{\lambda,k} = \xi\hbar v_t k_y + \lambda\hbar\sqrt{v_x^2k_x^2 + v_y^2k_y^2}, \tag{2}$$

where $\lambda = \pm$ is the band index and the 2D momentum vector is given by $\mathbf{k} = \{k_x,k_y\}$. The energy dispersion for the K valley is shown in Fig. 1, which is tilted along k_y due to the presence of the v_t term. In the K' valley, dispersion will be identical except the tilting is in the opposite direction. In addition to this, Dirac cones are anisotropic, which is in contrast to graphene. Note that because of the tilted feature of the Dirac cones, particle-hole symmetry is broken in borophene.

A. Inclusion of magnetic field

The perpendicular magnetic field ($\mathbf{B} = B\hat{z}$) is incorporated via the Landau-Peierls substitution as $\mathbf{p} \to \mathbf{p} + \mathbf{eA}$ in the low-energy single-electron effective Hamiltonian of borophene, lying in the x-y plane, as

$$\mathcal{H} = \xi[v_x p_x\sigma_x + v_y(p_y + eBx)\sigma_y + v_t(p_y + eBx)\sigma_0], \tag{3}$$

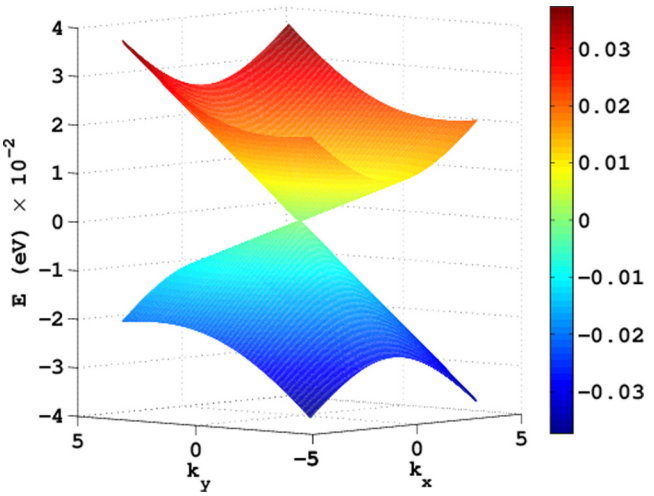

FIG. 1. The energy-band dispersion in k space representing Eq. (2). The momentum vectors are normalized by $k_0 = 10^7/\text{m}$.

under the Landau gauge $\mathbf{A} = (0,xB,0)$. Here, A is the magnetic vector potential. The commutator relation $[\mathcal{H},p_y] = 0$ guarantees the free particle nature of electrons along the y direction. Using this fact, the above Hamiltonian reduces to

$$\mathcal{H} = \xi\left\{\frac{\hbar v_t}{l_c}X\sigma_0 + \frac{\hbar v_c}{l_c}\left[\sqrt{\frac{v_x}{v_y}}\sigma_x P + \sqrt{\frac{v_y}{v_x}}\sigma_y X\right]\right\}, \tag{4}$$

where $l_c = \sqrt{\hbar/eB}$ is the magnetic length, $P = -i\partial/\partial(x/l_c)$, $v_c = \sqrt{v_x v_y}$, and $X = (x + x_0)/l_c$ with the center of cyclotron orbit at $x = -x_0 = -k_y l_c^2$. The above Hamiltonian is now similar to the case of monolayer graphene under a crossed electric and magnetic field [39] except the velocity anisotropy inside the third bracket. The first term is analogous to a pseudo in-plane effective electric field $E_{\text{eff}} = \xi\hbar v_t/(el_c^2)$. The typical values of the pseudoelectric field are $(320 \times B)$ kV. Now Eq. (4) can be rewritten as

$$\mathcal{H} = eE_{\text{eff}}(x + x_0)\sigma_0 + \xi\hbar\omega_c\begin{bmatrix} 0 & -ia \\ ia^\dagger & 0 \end{bmatrix}, \tag{5}$$

where $\omega_c(= v_c/l_c)$ is the cyclotron frequency and ladder operators are defined as $a = (\tilde{X} + i\tilde{P})/\sqrt{2}$ and $a^\dagger = (\tilde{X} - i\tilde{P})/\sqrt{2}$. Here, $\tilde{X} = \sqrt{\frac{v_y}{v_x}}X$ and $\tilde{P} = \sqrt{\frac{v_x}{v_y}}P$, which satisfy the commutator relation $[\tilde{X},\tilde{P}] = i$. In the absence of E_{eff}, the above Hamiltonian can be diagonalized to obtain graphenelike LLs

$$E_\zeta = \lambda\hbar\omega_c\sqrt{2n} \tag{6}$$

and eigenfunctions as

$$\psi_\zeta(\mathbf{r}) = \frac{e^{ik_y y}}{\sqrt{2L_y}}\begin{bmatrix} \lambda\phi_n(X) \\ -i\xi\phi_{n-1}(X) \end{bmatrix}, \tag{7}$$

where $\zeta = \{n,k_y\}$ and $\phi_n(X)$ is the well-known simple harmonic oscillator wave function. In the presence of E_{eff}, direct diagonalization of the above Hamiltonian is difficult. However, there is a standard way, given by Lukose *et al.* in Ref. [39], to solve this problem exactly. An alternative approach to solving this problem in graphene was also given by Peres and Castro [40]. Following Ref. [39], we transform the above Hamiltonian into a moving frame along the y direction with velocity $V = E_{\text{eff}}/B = v_t$, where the transformed electric field vanishes and the magnetic field reduces to $B' = B\sqrt{1 - \beta_b^2}$. Here, $\beta_b = v_t/\sqrt{v_x v_y}(= 0.4154)$ is termed as "tilt parameter." Note that the role of the velocity of light is played by v_c in borophene, whereas in graphene it is v_F. In the moving frame, LLs can be obtained as $\tilde{E}_{n,\tilde{k_y}} = \hbar\omega_c\sqrt{2n}(1 - \beta_b^2)^{1/4}$. However, required LLs and eigenstates in the rest frame can be obtained by Lorentz boost back transformation as [39,41]

$$E_\zeta = \lambda\hbar\omega_c\sqrt{2n}\left(1 - \beta_b^2\right)^{3/4}, \tag{8}$$

where the argument of the wave functions becomes

$$X' = \frac{\left(1 - \beta_b^2\right)^{1/4}}{l_c}\left[x + k_y l_c^2 + \lambda\frac{\sqrt{2n}l_c\beta_b}{\left(1 - \beta_b^2\right)^{1/4}}\right] \tag{9}$$

after using the Lorentz back transformation of momentum, giving the wave function in rest frame as

$$\Psi_\zeta(\mathbf{r}) = \frac{e^{ik_y y}}{\sqrt{2L_y\gamma}}\left[\begin{pmatrix}\cosh(\theta/2)\\ -i\sinh(\theta/2)\end{pmatrix}\lambda\phi_n(X') - i\xi\begin{pmatrix}i\sinh(\theta/2)\\ \cosh(\theta/2)\end{pmatrix}\phi_{n-1}(X')\right] \tag{10}$$

with $\tanh\theta = \beta_b$ and $\cosh\theta = \gamma$. Here, we have used the form of hyperbolic rotation matrix as

$$e^{-(\theta/2)\sigma_y} = \begin{bmatrix}\cosh(\theta/2) & i\sinh(\theta/2)\\ -i\sinh(\theta/2) & \cosh(\theta/2)\end{bmatrix}. \tag{11}$$

On the other hand, the LLs of graphene under the in-plane real electric field (E_r) is given by [39]

$$E_\zeta^g = \lambda\hbar\omega_c\sqrt{2n}\left(1-\beta_g^2\right)^{3/4} - \hbar k_y\frac{E_r}{B}, \tag{12}$$

where $\beta_g = \frac{E_r/B}{v_F}$ with v_F the Fermi velocity. Note that in cyclotron frequency, v_c should be replaced by v_F in graphene. In Eq. (8), β_b is a constant and acting like a system parameter, whereas β_g is tunable and governed by the strength of the in-plane electric field in graphene. As the tilt parameter (β_b) is constant, the LLs are protected from being collapsed in borophene, which is in contrast to graphene where LLs may get collapsed under the suitable strength of the electric field (i.e., when β_g becomes 1). Note that the LLs in borophene, derived in Eq. (8), exhibit k_y degeneracy, whereas in graphene [see Eq. (12)] this degeneracy is removed under the influence of an in-plane electric field. This is because the in-plane electric field in graphene gives rise to the potential energy as eEx, whereas in borophene for pseudoelectric field it is $eE_{\text{eff}}(x + x_0)$. The idea of relativistic Lorentz boost transformation was also used in an organic compound α-(BEDT-TTF)$_2I_3$ [42], exhibiting quite similar band structure.

The LLs, derived in Eq. (8), show that the tilt parameter (β_b) renormalizes each LL, which should be reflected in the longitudinal conductivity oscillations. Before going into conductivity, we now discuss how Fermi energy and DOS are affected by the tilting of the Dirac cones.

B. Fermi energy and density of states

In this section, we compute the Fermi energy (E_F) and DOS in terms of the tilt parameter and the magnetic field. In the presence of the magnetic field, the Fermi energy can be obtained by solving the following equation self-consistently:

$$n_e = \int_{-\infty}^{\infty} D(E)f(E)dE, \tag{13}$$

where

$$D(E) = \frac{g_s g_v}{\Omega}\sum_\zeta \delta(E - E_\zeta) \tag{14}$$

is the DOS per unit energy and per unit area. Here, g_s and g_v are the spin and valley degeneracy, respectively. Carrier density and the area of the system are denoted by n_e and $\Omega(= L_x L_y)$, respectively. The Fermi distribution function is given by $f(E) = (1 + \exp[(E - E_F)/k_B T])^{-1}$. The summation over

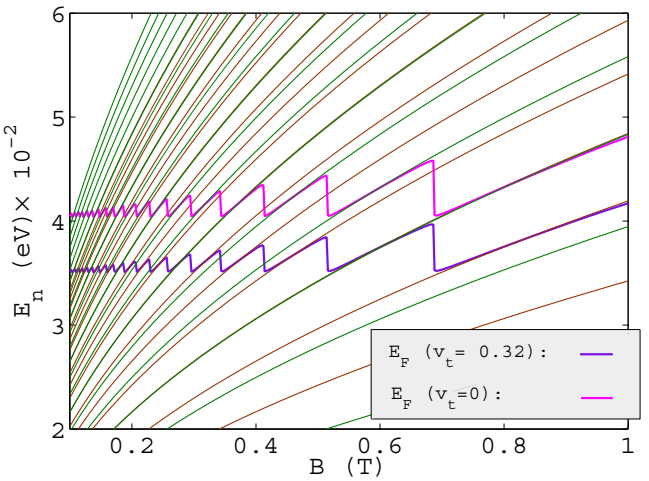

FIG. 2. The behavior of the Fermi energy and the LLs with magnetic field. For the plot of E_F versus B, we use $T = 1$ K and carrier density $n_e = 10^{15}m^{-2}$. Green and gray solid lines denote the first 20 LLs with and without v_t, respectively.

k_y can be computed by using the fact that the center of cyclotron orbit is always restricted by the system dimension, i.e., $0 \leqslant |x_0 + G_n| \leqslant L_x$ or $0 \leqslant k_y \leqslant L_x/l_c^2$. Then we can replace $\sum_{k_y} \to \frac{L_y}{2\pi}\int_0^{L_x/l_c^2} dk_y = \Omega/(2\pi l_c^2)$, known as k_y degeneracy. The factor $L_y/(2\pi)$ preserves the periodic boundary condition. Using these, finally Eq. (13) simplifies to

$$\pi n_e l_c^2 = 2\sum_n f(E_n), \tag{15}$$

which is solved numerically to plot the Fermi energy as a function of the magnetic field in Fig. 2. Here we have also substituted spin and valley degeneracy as $g_s = 2$ and $g_v = 2$, respectively. In the same plot, the first 20 LLs are also shown. The Fermi level is found to be fluctuating between two successive LLs with the variation of the magnetic field. The amplitude of fluctuation increases with the increase of the magnetic field, because of the increasing LLs spacing. To understand how the tilting feature of the Dirac cones affects the Fermi energy, we consider the two cases, i.e., when $v_t = 0$ and $v_t = 0.32$ units. It can be seen that for the same carrier density, the tilt factor (v_t) actually lowers the Fermi level. On the other hand, it causes a shift in the LLs as can be seen from Eq. (8). Note that the position of the jumping of Fermi level between two successive Landau levels remains unchanged in both cases.

Now we will examine the effects of the tilting of the Dirac cones on the behavior of the DOS in borophene. To plot the behavior of the DOS, we assume impurity- induced Gaussian broadening of the LLs and hence Eq. (14) reduces to

$$D(E) = D_0\sum_n \exp\left[-\frac{(E - E_n)^2}{2\Gamma_0^2}\right], \tag{16}$$

where

$$D_0 = \frac{g_s g_v}{2\pi l_c^2}\frac{1}{\Gamma_0\sqrt{2\pi}}. \tag{17}$$

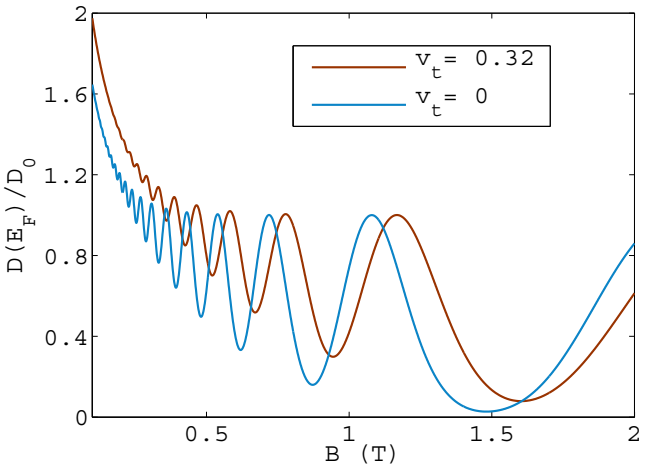

FIG. 3. DOS versus magnetic field. The Fermi energy $E_F = 0.035$ and 0.041 eV for $v_t = 0.32$ and 0 in units of v_0, respectively, as noted from Fig. 2.

The DOS is plotted in Fig. 3 by using Eq. (16). It is an established fact [43,44] that the impurity-induced LLs broadening in 2D Dirac material is directly proportional to $\sqrt{B}$. To plot dimensionless DOS, we consider LLs broadening width $\Gamma_0 = 0.1\hbar\omega_c$. To explore the effects of the tilted Dirac cone, we consider both cases, i.e., with and without v_t. The DOS shows oscillation with the magnetic field, known as SdH oscillation. The presence of v_t is causing a significant impact on the frequency of the SdH oscillations. It is also observed that below a certain magnetic field, the SdH oscillation vanishes because of the reduction in the LLs spacing and overlapping of the LLs to each other due to the impurity-induced broadening.

III. MAGNETOCONDUCTIVITY

In this section, we evaluate magnetoconductivity in the presence of a periodic electric/magnetic modulation at low magnetic field regime. In the presence of a spatial electric/magnetic modulation along the x direction, the electron gains a finite drift velocity along the y direction for which an additional contribution to the y component of the longitudinal conductivity appears, known as diffusive conductivity [17], i.e., $\sigma_{yy} = \sigma_{yy}^{\rm dif} + \sigma_{xx}^{\rm col}$. Here, $\sigma_{xx}^{\rm col}$ is the collisional conductivity which arises due to LL-induced oscillatory DOS without any external modulation, whereas $\sigma_{yy}^{\rm dif}$ is the diffusive conductivity that arises because of the modulation. On the other hand, the longitudinal conductivity along the x direction is $\sigma_{xx} = \sigma_{xx}^{\rm col}$ because $\sigma_{xx}^{\rm dif} = 0$. However, in this work our major focus will be modulation-induced diffusive conductivity which can be evaluated by [17,45]

$$\sigma_{\mu\nu}^{\rm dif} = \frac{\beta e^2}{\Omega}\sum_{\zeta} f_\zeta(1-f_\zeta)\tau(E_\zeta)\mathcal{V}_\mu\mathcal{V}_\nu \tag{18}$$

provided the scattering processes are elastic or quasielastic. Here, $f_\zeta = [1+\exp\{\beta(E_\zeta - E_F)\}]^{-1}$ is the Fermi-Dirac distribution function with $\beta = (k_B T)^{-1}$ where k_B is the Boltzmann constant. In the above formula, $\tau(E_\zeta)$ denotes the energy-dependent collision time and the group velocity $\mathcal{V}_{\mu(\nu)} = (1/\hbar)\partial E_\zeta/\partial k_{\mu(\nu)}$. In general, the electron does not possess any nonzero drift velocity inside the bulk, i.e., $\mathcal{V}_x = \mathcal{V}_y = 0$. However, the application of a spatial electric/magnetic modulation can induce a nonzero finite drift velocity and concurrently gives rise to the diffusive conductivity as discussed below.

A. Electric modulation

The application of a weak electric modulation to the borophene sheet is described by the total Hamiltonian $\mathcal{H}_T^e = \mathcal{H} + V_e\sin(\Lambda x)$, where V_e is the modulation strength and $\Lambda = 2\pi/a$ with a is the period. Using perturbation theory, we evaluate the first-order energy correction as

$$\Delta E_\zeta^e = \int_0^{L_y} dy \int_{-\infty}^{\infty} \Psi_\zeta^\dagger(\mathbf{r}) V_e \sin(\Lambda x)\Psi_\zeta(\mathbf{r})dx$$
$$= \frac{V_e}{2}[\xi\beta_b R_n(u)\cos(\Lambda\bar{x}_0) - F_n(u)\sin(\Lambda\bar{x}_0)]. \tag{19}$$

Here $\bar{x}_0 = x_0 + G_n$ with $G_n = \sqrt{2n\gamma}l_c\beta_b$. Also,

$$F_n(u) = e^{-u/2}[L_{n-1}(u) + L_n(u)] \tag{20}$$

and

$$R_n(u) = \sqrt{\frac{8n}{u}}e^{-u/2}[L_{n-1}(u) - L_n(u)], \tag{21}$$

where $L_n(u)$ is the Laguerre polynomial of order n and $u = \gamma\Lambda^2 l_c^2/2$ with $\gamma = (1-\beta_b^2)^{-1/2}$. The total energy is now $E_\zeta^e = E_\zeta + \Delta E_\zeta^e$ where k_y degeneracy is now lifted. The presence of modulation broadens the LLs width by contributing additional energy ΔE_ζ^e. The width of the LLs broadening, i.e., bandwidth (in units of V_e) is given by $\Delta_e = \sqrt{|\beta_b R_n(u)|^2 + |F_n(u)|^2}$, which is oscillatory [17] with the inverse magnetic field, as the Laguerre polynomial exhibits an oscillatory feature. Note that the first term in Eq. (19) is purely due to the tilting of the Dirac cones which simply vanishes with the tilting parameter $\beta_b = 0$. On the other hand, the second term in the first-order energy correction is analogous to the monolayer graphene case [31].

Now the drift velocity $\mathcal{V}_{\mu(\nu)}$ is obtained as

$$\mathcal{V}_y = -\frac{V_e}{\hbar\Lambda}\frac{u}{\gamma}[\xi\beta_b R_n(u)\sin(\Lambda\bar{x}_0) + F_n(u)\cos(\Lambda\bar{x}_0)] \tag{22}$$

and $\mathcal{V}_x = 0$, which suggests that the diffusive conductivity arises along the transverse direction to the applied modulation. Now, after inserting $\mathcal{V}_y$ into Eq. (18), we obtain diffusive conductivity as

$$\sigma_{yy}^e = \frac{e^2}{h}\frac{V_e^2}{4\Gamma_0}\frac{u}{\gamma}\sum_n\left[-\frac{\partial f_n}{\partial E}\right]\{[F_n(u)]^2 + [\beta_b R_n(u)]^2\}, \tag{23}$$

where Γ_0 is the impurity-induced broadening. Here, we assume that the collisional time $\tau(E_\zeta)$ is very insensitive to the energy, i.e., $\tau(E_\zeta) \simeq \tau_0$, which is a good approximation under low magnetic field regime. We have also substituted $\Gamma_0 \approx \hbar/\tau_0$. The major effects of modulation arise via nonzero drift velocity. On the other hand, the modulation effect on Fermi distribution function is very small, and hence we ignore it. The diffusive conductivity in the above Eq. (23) is oscillatory with magnetic field because of the oscillatory nature of the bandwidth (Δ_e). This oscillation is known as Weiss oscillation.

For the numerical plots, we use the following physical parameters: modulation period $a = 350$ nm, charge density $n_e = 10^{15}m^{-2}$, and temperature $T = 3$ K. The diffusive conductivity for the electric modulation is plotted with inverse magnetic field in Fig. 4(a). To explore the effects of the tilted Dirac cones, we consider both situations, i.e., $v_t = 0$ and $v_t = 0.32$ units. The diffusive conductivity exhibits the Weiss oscillation at low magnetic field regime with the inverse magnetic field. However, with the increase of the magnetic field, SdH oscillations start to superimpose over the Weiss oscillation. The SdH oscillations appear as small oscillations over the envelope of the Weiss oscillation. The tilted Dirac cones cause a significant change in the frequency of the Weiss oscillation too. To understand the effect of tilting Dirac cones more explicitly, we shall obtain an approximate analytical expression of the diffusive conductivity. Following Refs. [31,33], the diffusive conductivity for electric modulation can be simplified to an analytical form by using the higher Landau-level approximation

$$e^{-u/2}L_n(u) \to \frac{1}{\sqrt{\pi\sqrt{nu}}}\cos\left(2\sqrt{nu} - \frac{\pi}{4}\right) \tag{24}$$

as

$$\sigma^e_{yy} \simeq \frac{e^2}{h}\frac{\beta_W}{8\pi^2\Gamma_0\gamma}\left\{U^e_0 - U^e_1 R^W\left(\frac{T}{T_W}\right) + 2R^W U^e_1\left(\frac{T}{T_W}\right) \times \cos^2\left[2\pi\left(\frac{f}{B} - \frac{1}{8}\right)\right]\right\}. \tag{25}$$

Here, $U^e_0 = (V_e)^2(1 + 2\beta_b^2)$ and $U^e_1 = V_e^2(2\beta_b^2 - 1)$. The amplitude of the conductivity is governed by U^e_0, which indicates that it enhances with the tilting of Dirac cones. On the other hand, the Weiss oscillation amplitude is determined by the factor U^e_1 which is suppressed by the tilting feature of the Dirac cones. The frequency of the Weiss oscillation is given by $f = E_F\gamma^2/(ev_c a)$. It is clearly seen that the frequency is enhanced by a tilt-dependent term $\gamma^2 = 1.20$. Note that in comparison to graphene, it is not only the tilt parameter which enhances the frequency of the Weiss oscillation, but also the Fermi velocity ($v_c = 0.77 \times 10^6$ m/sec) which is smaller than its counterpart in graphene ($v_F = 3 \times 10^6$ m/s). Also, $\beta_W = (k_B T_W)^{-1}$ with the characteristic temperature $T_W = eav_c B/[4(\pi\gamma)^2 k_B]$ which is lowered by the tilt parameter. The temperature also induces a damping to the Weiss oscillation amplitude, which is described by

$$R^W\left(\frac{T}{T_W}\right) = \frac{T/T_W}{\sinh(T/T_W)}. \tag{26}$$

B. Magnetic modulation

Now we consider the case when the perpendicular magnetic field is weakly modulated without any electrical modulation. The underlying physics of the charge carriers in the presence of a modulated magnetic field is believed to be closely related to *composite fermions* in the fractional quantum Hall regime [46]. Under the weak magnetic field and low temperature regime, extensive theoretical works of the Weiss oscillation exist from usual 2DEG to monolayer graphene (as mentioned in Sec. I). Along the same line, we investigate Weiss oscillation in a magnetically modulated borophene.

First, we evaluate the first-order energy correction due to magnetic modulation. Let the perpendicular magnetic field be modulated very weakly as $\mathbf{B} = [B + B_m\cos(\Lambda x)]\hat{z}$, where $B_m \ll B$ describes the vector potential under the Landau gauge $\mathbf{A} = [0, Bx + (B_m/\Lambda)\sin(\Lambda x)]$. Similar to the case of electric modulation, the total Hamiltonian can now be split into two parts as $\mathcal{H}^m_T = \mathcal{H} + \mathcal{H}_m$, where $\mathcal{H}$ is the unperturbed Hamiltonian and $\mathcal{H}_m$ is the modulation-induced perturbation which can be written as

$$\mathcal{H}_m = \xi\frac{eB_m\sin(\Lambda x)}{\Lambda}(\sigma_0 v_t + \sigma_y v_c). \tag{27}$$

Using the unperturbed wave function, the first-order energy correction due to the magnetic modulation $\mathcal{H}_m$ is evaluated as

$$\Delta E^m_\zeta = \tfrac{1}{2}\left[\xi V^{ct}_m F_n(u)\sin(\Lambda\bar{x}_0) + V^{tc}_m R_n(u)\cos(\Lambda\bar{x}_0)\right]. \tag{28}$$

Here, $V^{ct}_m = (\beta_b V^c_m - V^t_m)$ and $V^{tc}_m = (\beta_b V^t_m - V^c_m)$ with $V^t_m = eB_m v_t/\Lambda$ and $V^c_m = eB_m v_c/\Lambda$. In the above energy correction, in Eq. (28), the terms involving V^t_m and β_b are purely due to the tilting feature of the Dirac cones. The above equation can be reduced to the case of magnetically modulated graphene [33] by setting $\beta_b = V^t_m = 0$. The width of the LLs broadening is $\Delta_m = \sqrt{[V^{ct}_m F_n(u)]^2 + [V^{tc}_m R_n(u)]^2}$. Now the group velocity is found to be

$$\mathcal{V}_y = \frac{u}{\hbar\gamma\Lambda}\left[\xi V^{ct}_m F_n(u)\cos(\Lambda\bar{x}_0) - V^{tc}_m R_n(u)\sin(\Lambda\bar{x}_0)\right] \tag{29}$$

and $\mathcal{V}_x = 0$. Following the same procedure, as in the electric modulation case, we obtain the diffusive conductivity as

$$\sigma^m_{yy} = \frac{e^2}{h}\frac{u}{4\gamma\Gamma_0}\sum_n\left[-\frac{\partial f_n}{\partial E}\right]\left\{\left[V^{ct}_m F_n(u)\right]^2 + \left[V^{tc}_m R_n(u)\right]^2\right\}. \tag{30}$$

Note that the diffusive conductivities for electrically [Eq. (23)] and magnetically modulated [Eq. (30)] borophene are independent of the valley index. The first term inside the third set of brackets in the above equation arises due to the tilting of the Dirac cones, and gives extra contribution to the diffusive conductivity. Following s similar approach as in the electric modulation case, we obtain the analytical expression of diffusive conductivity as

$$\sigma^m_{yy} \simeq \frac{e^2}{h}\frac{\beta_W U_0}{8\pi^2\gamma\Gamma_0}\left\{1 - \left(\frac{U_1}{U_0}\right)R^W\left(\frac{T}{T_W}\right) + 2\left(\frac{U_1}{U_0}\right)R^W\left(\frac{T}{T_W}\right)\sin^2\left[2\pi\left(\frac{f}{B} - \frac{1}{8}\right)\right]\right\} \tag{31}$$

with $U_0 = (V^{ct}_m)^2 + (\sqrt{2}V^{tc}_m)^2$ and $U_1 = (\sqrt{2}V^{tc}_m)^2 - (V^{ct}_m)^2$. The amplitude of the Weiss oscillations is governed by the factor U_1 and it is suppressed in the presence of the tilt-induced term V^t_m. The tilt-induced additional contribution to the diffusive conductivity does not appear in nontilted Dirac material graphene.

The diffusive conductivity for magnetic modulation is plotted numerically in Fig. 4(b), where Weiss oscillation is

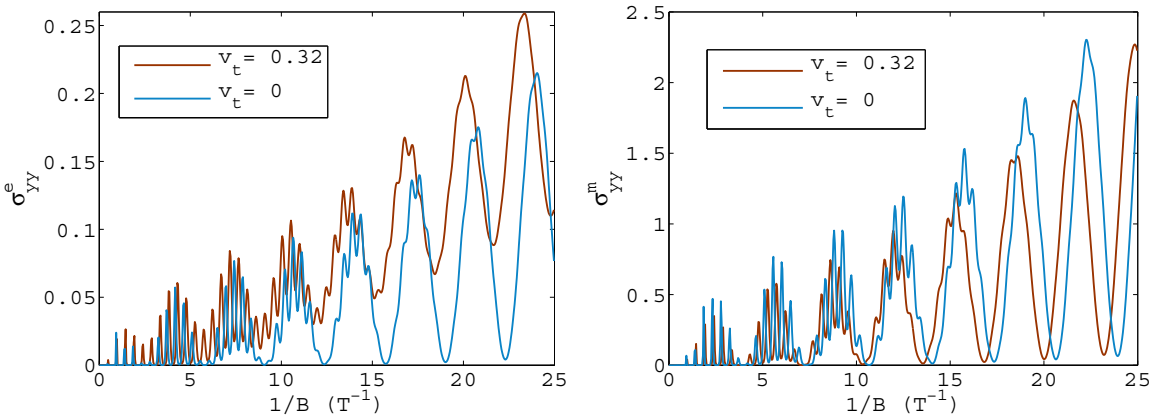

FIG. 4. Diffusive conductivity (in units of e^2/h) versus inverse magnetic field for (a) electric and (b) magnetic modulation. The Fermi energy is taken as 0.041 and 0.035 eV for $v_t = 0$ and 0.32 in units of v_0, respectively. The modulation period is $a = 350$ nm and temperature $T = 3$ K. The strength of modulation is $V_e = 0.5$ meV. The strength of the magnetic modulation is taken as $B_m = 0.028$ T, such that $V_m^t = V_e$.

found to be weakly suppressed. The origin of this suppression can be understood from the analytical expression of diffusive conductivity given in Eq. (31). The presence of the tilt-induced term V_m^t reduces the amplitude of the oscillation, governed by U_1. Note that we have taken the strength of magnetic modulation $B_m = 0.028$ T, such that $V_e = V_m^t = 0.5$ meV and $V_m^c = 1.2$ meV. Note that, in comparison to the case of electrical modulation, the amplitude of Weiss oscillation is enhanced.

C. Presence of both modulations

Now we consider the situation when both types of modulation, i.e., electric and magnetic, are present together. The presence of both modulations may give rise to some new features to the Weiss oscillation. In usual 2DEG [19], it was found that Weiss oscillation can be pronounced or suppressed depending on whether both modulations are in phase or out of phase. Recently, we have observed that the presence of both modulations can break particle-hole symmetry in Dirac materials like graphene and α-T_3 lattice [37]. First we consider that the electric and magnetic modulations are out of phase, i.e., $V_e \sin(\Lambda x)$ and $B_m \cos(\Lambda x)$, respectively. The total first-order energy correction is evaluated to be

$$\Delta E_\zeta^{em} = \tfrac{1}{2}\left[W_1^\xi R_n(u)\cos(\Lambda\bar{x}_0) + W_2^\xi F_n(u)\sin(\Lambda\bar{x}_0)\right], \quad (32)$$

where $W_1^\xi = (\xi V_e\beta_b + V_m^{tc})$ and $W_2^\xi = (\xi V_m^{ct} - V_e)$. The group velocity of charge carriers under the combined effects of both modulations out of phase is evaluated as

$$\mathcal{V}_y = \frac{u}{\hbar\gamma\Lambda}\left[W_2^\xi F_n(u)\cos(\Lambda\bar{x}_0) - W_1^\xi R_n(u)\sin(\Lambda\bar{x}_0)\right] \quad (33)$$

and $\mathcal{V}_x = 0$. Following the same procedure as in the case of electric/magnetic modulation, we obtain the valley-dependent diffusive conductivity as

$$\sigma_{yy}^\xi \simeq \frac{e^2}{h}\frac{\beta_W u}{8\gamma\Gamma_0}\sum_n\left[-\frac{\partial f_n}{\partial E}\right]\left\{\left[W_1^\xi R_n(u)\right]^2 + \left[W_2^\xi F_n(u)\right]^2\right\}. \quad (34)$$

The most remarkable point here is that now the diffusive conductivity is very sensitive to the valley index and can cause sizable valley polarization, which is attributed to the presence of the tilt-induced term V_m^t and β_b. In nontilted Dirac cones like graphene, valley polarization does not appear even in the presence of both modulations because of the absence of the terms V_m^t and β_b. Using a similar approach as in the electric/magnetic modulation, the analytical form of the diffusive conductivity can be obtained as

$$\sigma_{yy}^\xi = \frac{e^2}{h}\frac{\beta_W U_0^\xi}{16\pi^2\gamma\Gamma_0}\left\{1 - \left(\frac{U_1^\xi}{U_0^\xi}\right)R^W\left(\frac{T}{T_W}\right) + 2\left(\frac{U_1^\xi}{U_0^\xi}\right)R^W\left(\frac{T}{T_W}\right)\sin^2\left[2\pi\left(\frac{f}{B} - \frac{1}{8}\right)\right]\right\}, \quad (35)$$

where $U_0^\xi = (W_1^\xi)^2 + (W_2^\xi)^2$ and $U_1^\xi = (W_1^\xi)^2 - (W_2^\xi)^2$. The amplitude of the Weiss oscillation is determined by a valley-dependent factor U_1^ξ. In the K valley ($\xi = +$), the Weiss oscillation amplitude is much more suppressed than in the K' valley ($\xi = -$), which is shown in the lower panel of Fig. 5. The upper panel of this figure shows that when electric and magnetic modulations are applied individually, the Weiss oscillation in one valley (K or K') exhibits opposite phase with an amplitude mismatch. The origin of the opposite phase is well addressed in Ref. [33]. However, when both modulations are applied together the two valleys respond differently. The Weiss oscillation amplitudes are enhanced in both valleys but the enhancement in the K' valley is much higher than in the K valley, as shown in the lower panel of Fig. 5. These features can be understood from the analytical expression of diffusive conductivity in Eq. (35). In the K valley, the amplitude of Weiss oscillation is determined by U_1^+, which is smaller than its counterpart in the K' valley, i.e., U_1^-.

On the other hand, if we consider that both modulations are in the same phase, i.e., electric modulation is $V_e\cos(\Lambda x)$ and the magnetic modulation is of the form of $B_m\cos(\Lambda x)$, then

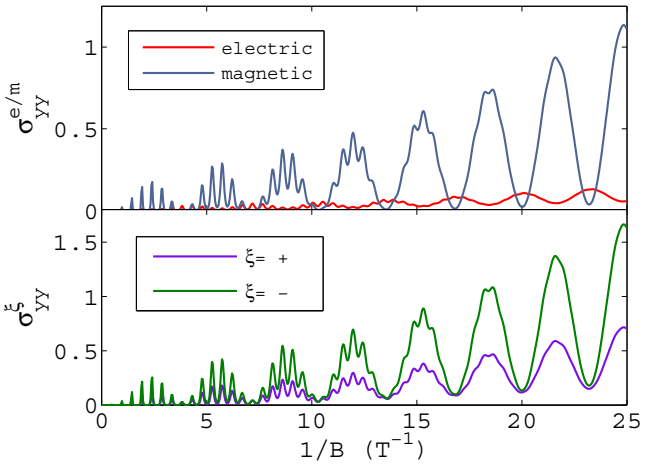

FIG. 5. Diffusive conductivity (in units of e^2/h) versus inverse magnetic field for electric and magnetic modulation (upper panel) and in the presence of both out-of-phase modulations (lower panel) in each valley. The tilt velocity $v_t = 0.32v_0$ and Fermi energy is 0.035 eV. All other parameters are the same as in Fig. 4.

diffusive conductivity will be

$$\sigma^{em}_{yy} = \frac{e^2}{h}\frac{u}{4\gamma\Gamma_0}\sum_n\left[-\frac{\partial f_n}{\partial E}\right]\{[W_3(n,u)]^2 + [W_4(n,u)]^2\}, \tag{36}$$

where $W_3(n,u) = [V_e\beta_b R_n(u) + V_m^{ct}F_n(u)]$ and $W_4(n,u) = [V_m^{ct}R_n(u) - V_e F_n(u)]$. In this case, diffusive conductivity does not depend on the valley index. A similar analytical expression can also be found by following the same approach. The Weiss oscillations for the presence of both in-phase and out-of phase modulations are presented together in Fig. 6, which shows that the Weiss oscillations in both cases are in opposite phase with amplitude mismatch. This feature is the direct consequence of the total effective energy correction in both cases. As we have seen that the diffusive conductivity

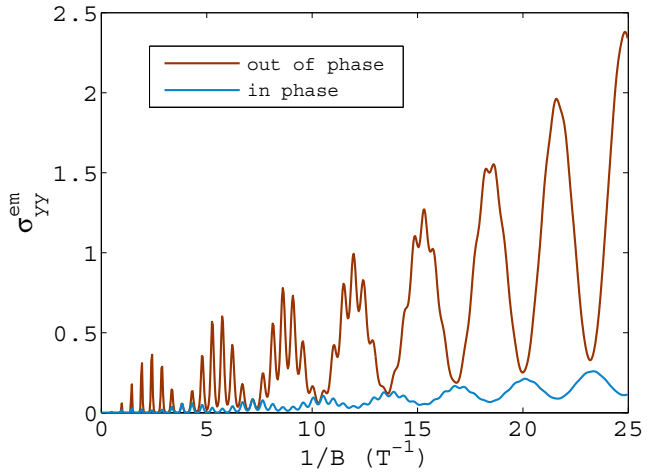

FIG. 6. Diffusive conductivity (in units of e^2/h) versus inverse magnetic field in the presence of both modulations. All other parameters are kept the same as in Fig. 5.

may be sensitive to the valley index depending on the phase relationship between electric and magnetic modulations, it is interesting to examine the valley polarization, for which we plot it versus inverse magnetic field in Fig. 7. Because of the unequal suppression of Weiss oscillations in two valleys in the presence of out of phase both modulations, a sizeable valley polarization arises in the diffusive conductivity. To plot valley polarization, we define it as

$$P_v = \frac{\sigma^+_{yy} - \sigma^-_{yy}}{\sigma^+_{yy} + \sigma^-_{yy}}. \tag{37}$$

The valley polarization oscillates with the inverse magnetic field with the frequency of Weiss oscillation as shown in Fig. 7(a). The appearance of valley polarization strongly depends on the phase relationship between both modulations. Valley polarization appears in Weiss oscillation only when electric and magnetic modulations are in out of phase. It is also interesting to examine the evolution of valley polarization with v_t. In Fig. 7(b), we also show the evolution of valley polarization in diffusive conductivity with the smooth variation of tilt velocity v_t. It shows that valley polarization oscillates with v_t, which can be easily understood from the fact that Weiss oscillation frequency has a strong dependency on v_t too. The valley polarization shows the emergence of regular peaks with increasing height toward 1 with the increase of v_t. We mention here that we have taken Fermi energy (0.035 eV) as constant while plotting Fig. 7(b) although a weak dependency of Fermi energy on v_t exists as shown in Fig. 2. The rise of valley-polarized Weiss oscillation in diffusive conductivity is one of our main results which differs from graphene. Here, we mention that the valley-polarized Weiss oscillation was predicted in electrically modulated silicene [36] too. However, in that case a gate voltage between two planes of sublattices is necessary in addition to the strong spin-orbit interaction.

Finally, we discuss whether tilt parameter can be extracted from the Weiss oscillation experiment. The frequency of the Weiss oscillation can be easily obtained from magnetoresistance measurement of borophene, which can be directly used to extract the tilt parameter once we know the Fermi level and Fermi velocity. The direct method of obtaining Fermi level and velocity was recently reported in Ref. [47].

IV. SUMMARY AND CONCLUSIONS

In this work, we have studied the magnetotransport properties of a 2D sheet of the polymorph of a periodically modulated 8-$Pmmn$ borophene which exhibits tilted anisotropic Dirac cones. We have evaluated the modulation-induced diffusive conductivity by using the linear response theory. The diffusive conductivity exhibits the Weiss oscillation with the inverse magnetic field, the frequency of which is enhanced by the tilted feature of the Dirac cones. The amplitude of Weiss oscillation is also enhanced or suppressed depending on the types of modulation. Most remarkably, we have found that the presence of out-of phase electric and magnetic modulations can cause very high valley polarization in Weiss oscillation at low magnetic field. The appearance of the valley polarization in the Weiss oscillation is the direct manifestation of the tilted

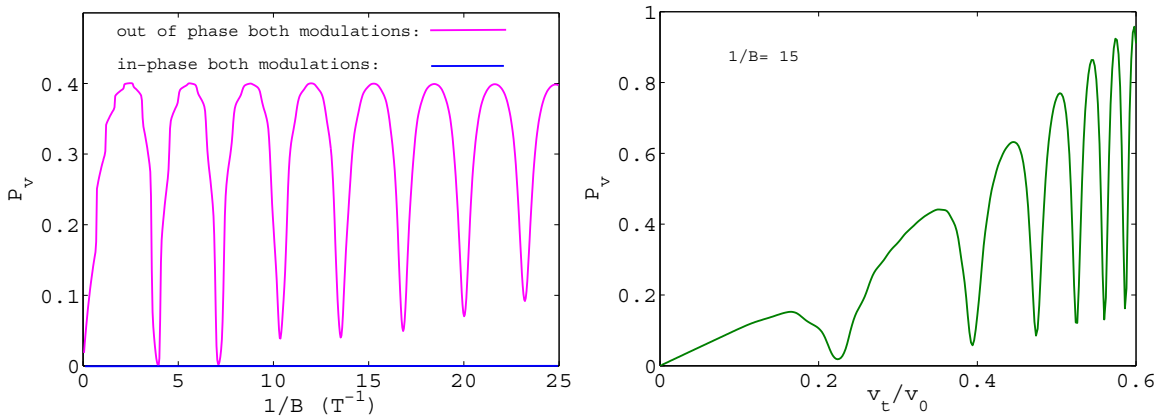

(a) (b)

FIG. 7. Valley polarization versus (a) inverse magnetic field and (b) tilt velocity (v_t). Fermi energy is kept fixed at $E_F = 0.035$ eV. All parameters are kept the same as Fig. 4.

Dirac cones in borophene. It is in complete contrast to the nontilted isotropic Dirac material graphene where such valley polarization does not appear.

As far as the practical realization of this material is concerned, a borophene structure can be formed on the surface of Ag(111) as reported recently in Ref. [4]. On the other hand, periodic modulation can be imparted to the system by several methods. For example, an array of biased metallic strips on the surface of a 2D electronic system has been used by Winkler *et al.* [14] to achieve electric modulation. Magnetic modulation can be generated by placing a few patterned ferromagnets or a superconductor on the surface of the 2D material [26–28].

ACKNOWLEDGMENTS

S.F.I. thanks T. K. Ghosh and T. Biswas for useful comments. The authors also thank the anonymous referee for pointing out an error in the calculation. A.M.J. acknowledges DST, India for support from a J.C. Bose National Fellowship.

[1] A. H. Castro Neto, F. Guinea, N. M. R. Peres, K. S. Novoselov, and A. K. Geim, Rev. Mod. Phys. **81**, 109 (2009).
[2] S. D. Sarma, S. Adam, E. Hwang, and E. Rossi, Rev. Mod. Phys. **83**, 407 (2011).
[3] X.-F. Zhou, X. Dong, A. R. Oganov, Q. Zhu, Y. Tian, and H.-T. Wang, Phys. Rev. Lett. **112**, 085502 (2014).
[4] B. Feng, O. Sugino, R.-Y. Liu, J. Zhang, R. Yukawa, M. Kawamura, T. Iimori, H. Kim, Y. Hasegawa, H. Li, L. Chen, K. Wu, H. Kumigashira, F. Komori, T.-C. Chiang, S. Meng, and I. Matsuda, Phys. Rev. Lett. **118**, 096401 (2017).
[5] A. Lopez-Bezanilla and P. B. Littlewood, Phys. Rev. B **93**, 241405 (2016).
[6] V. M. Pereira and A. H. Castro Neto, Phys. Rev. Lett. **103**, 046801 (2009).
[7] A. D. Zabolotskiy and Y. E. Lozovik, Phys. Rev. B **94**, 165403 (2016).
[8] K. Sadhukhan and A. Agarwal, Phys. Rev. B **96**, 035410 (2017).
[9] S. Verma, A. Mawrie, and T. K. Ghosh, Phys. Rev. B **96**, 155418 (2017).
[10] D. Feng and G. Jin, *Introduction to Condensed Matter Physics* (World Scientific, Singpore, 2005), Vol. 1.
[11] J. Imry, *Introduction to Mesoscopic Physics*, Mesoscopic Physics and Nanotechnology (Oxford University Press, New York, 1997).
[12] D. Weiss, K. Klitzing, K. Ploog, and G. Weimann, Europhys. Lett. **8**, 179 (1989).
[13] R. R. Gerhardts, D. Weiss, and K. v. Klitzing, Phys. Rev. Lett. **62**, 1173 (1989).
[14] R. W. Winkler, J. P. Kotthaus, and K. Ploog, Phys. Rev. Lett. **62**, 1177 (1989).
[15] P. Vasilopoulos and F. M. Peeters, Phys. Rev. Lett. **63**, 2120 (1989).
[16] C. Zhang and R. R. Gerhardts, Phys. Rev. B **41**, 12850 (1990).
[17] F. M. Peeters and P. Vasilopoulos, Phys. Rev. B **46**, 4667 (1992).
[18] C. W. J. Beenakker, Phys. Rev. Lett. **62**, 2020 (1989).
[19] F. M. Peeters and P. Vasilopoulos, Phys. Rev. B **47**, 1466 (1993).
[20] P. Vasilopoulos and F. Peeters, Superlattices Microstruct. **7**, 393 (1990).
[21] T.-Z. Li, S.-W. Gu, X.-H. Wang, and J.-P. Peng, J. Phys.: Condens. Matter **8**, 313 (1996).
[22] A. Matulis and F. M. Peeters, Phys. Rev. B **62**, 91 (2000).
[23] A. S. Mel'nikov, S. V. Mironov, and S. V. Sharov, Phys. Rev. B **81**, 115308 (2010).
[24] D. P. Xue and G. Xiao, Phys. Rev. B **45**, 5986 (1992).
[25] G. Papp and F. Peeters, J. Phys.: Condens. Matter **16**, 8275 (2004).
[26] S.-i. Izawa, S. Katsumoto, A. Endo, and Y. Iye, J. Phys. Soc. Jpn. **64**, 706 (1995).
[27] H. A. Carmona, A. K. Geim, A. Nogaret, P. C. Main, T. J. Foster, M. Henini, S. P. Beaumont, and M. G. Blamire, Phys. Rev. Lett. **74**, 3009 (1995).
[28] P. D. Ye, D. Weiss, R. R. Gerhardts, M. Seeger, K. von Klitzing, K. Eberl, and H. Nickel, Phys. Rev. Lett. **74**, 3013 (1995).
[29] X. F. Wang, P. Vasilopoulos, and F. M. Peeters, Phys. Rev. B **71**, 125301 (2005).

[30] S. F. Islam and T. K. Ghosh, J. Phys.: Condens. Matter **24**, 185303 (2012).
[31] A. Matulis and F. M. Peeters, Phys. Rev. B **75**, 125429 (2007).
[32] R. Nasir, K. Sabeeh, and M. Tahir, Phys. Rev. B **81**, 085402 (2010).
[33] M. Tahir and K. Sabeeh, Phys. Rev. B **77**, 195421 (2008).
[34] M. Zarenia, P. Vasilopoulos, and F. M. Peeters, Phys. Rev. B **85**, 245426 (2012).
[35] S. F. Islam and T. K. Ghosh, J. Phys.: Condens. Matter **26**, 335303 (2014).
[36] K. Shakouri, P. Vasilopoulos, V. Vargiamidis, and F. M. Peeters, Phys. Rev. B **90**, 125444 (2014).
[37] SK Firoz Islam and P. Dutta, Phys. Rev. B **96**, 045418 (2017).
[38] M. Tahir and P. Vasilopoulos, J. Phys.: Condens. Matter **29**, 425302 (2017).
[39] V. Lukose, R. Shankar, and G. Baskaran, Phys. Rev. Lett. **98**, 116802 (2007).
[40] N. Peres and E. V. Castro, J. Phys.: Condens. Matter **19**, 406231 (2007).
[41] J. Sári, M. O. Goerbig, and C. Tőke, Phys. Rev. B **92**, 035306 (2015).
[42] M. Goerbig, J.-N. Fuchs, G. Montambaux, and F. Piéchon, Europhys. Lett. **85**, 57005 (2009).
[43] Y. Zheng and T. Ando, Phys. Rev. B **65**, 245420 (2002).
[44] M. E. Raikh and T. V. Shahbazyan, Phys. Rev. B **47**, 1522 (1993).
[45] M. Charbonneau, K. Van Vliet, and P. Vasilopoulos, J. Math. Phys. **23**, 318 (1982).
[46] A. Endo, M. Kawamura, S. Katsumoto, and Y. Iye, Phys. Rev. B **63**, 113310 (2001).
[47] S. Kim, I. Jo, D. C. Dillen, D. A. Ferrer, B. Fallahazad, Z. Yao, S. K. Banerjee, and E. Tutuc, Phys. Rev. Lett. **108**, 116404 (2012).